Axial Lifetime Control by Radiation Induced Centers in Fast Recovery Diodes

R. Siemieniec [(1)] and J. Lutz [(2)]
[(1)] Department of Solid-State Electronics, Technical University of Ilmenau
[(2)] Faculty of Electrical Engineering and Information Technology, Technical University of Chemnitz
GERMANY

Abstract

Device simulation, based on an extended recombination model, is used as a design tool for lifetime-controlled power diodes with different lifetime profiles. Homogenous and local recombination center profiles are considered. The sensitivity of important device properties, such as the trade-off between stationary and dynamical characteristics, to the recombination center peak position is investigated. The occurrence of dynamic impatt oscillations is analyzed.

Keywords: lifetime control, irradiation, recombination, simulation, fast recovery diode, impatt oscillation

INTRODUCTION

The use of irradiation techniques for carrier lifetime control is nowadays a commonly accepted strategy for optimizing power device characteristics. In comparison with the conventionally used impurities gold and platinum, the irradiation techniques offer an exact process control and the possibility to realize different lifetime profiles. Today, irradiation-based lifetime adjustment steps are applied to a wide variety of power devices like IGBTs, GTOs and Freewheeling Diodes (FWDs).
The improvement and optimization of radiated devices was usually done through time- and cost-consuming experiments. Using a device simulation tool with an appropriate extended recombination model allows a significant reduction of the necessary experimental efforts. Based on center parameters determined in earlier work [11,12], the effects of different lifetime profiles on the stationary and dynamical characteristics of fast recovery diodes are studied in this work using 2D device simulation. The validity of the results is demonstrated by comparison with measurements taken on manufactured samples.

Type	Profile	Particles	Particle Energy
N	none	-	-
H	local	helium ions	5.4MeV
E	homogenous	electrons	1.1MeV
E45	homogenous	electrons	4.5MeV
E100	homogenous	electrons	10MeV
EH	homogenous and local	electrons and helium ions	1.1MeV 5.4MeV

Table 1: Overview of studied profile types

LIFETIME CONTROL

In this work, device simulation is used for the investigation of the influence of various lifetime profiles on the properties of fast silicon power diodes with a blocking voltage of 1.2kV. Table 1 gives an overview of the studied basic profile types. Additionally, the irradiation dose was varied. The parameters of the recombination centers, as given in Table 2, were determined in previos work [11,12]. All samples were annealed at identical conditions.

SIMULATION MODEL

Irradiation generates centers with different energy levels in the band gap of Silicon semiconductors. Each level may act as an effective recombination center where the total recombination rate results from the emission and capture processes of each single level as illustrated in Figure 1. The implementation of this extended model, which includes the complete trap dynamics, is fundamental for

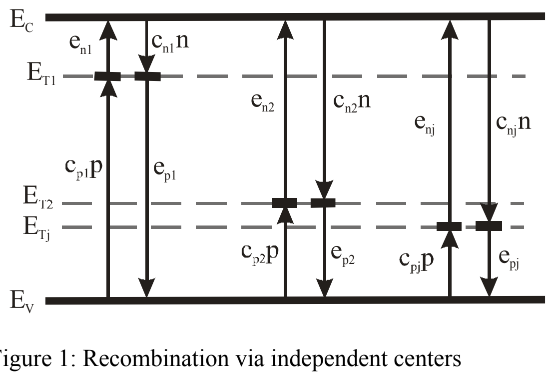

Figure 1: Recombination via independent centers

Trap	Energy level	Capture coefficients	
		c_n [cm³/s]	c_p [cm³/s]
E(90K)	E_C-E_T=0.167eV	$1.15\cdot 10^{-7}\exp\left(-\frac{T}{355.4K}\right)$	$6.39\cdot 10^{-7}\sqrt{\frac{T}{300}}\exp\left(\frac{6.15\cdot 10^{-3}}{k_B T}\right)$
E(230K)	E_C-E_T=0.447eV	$3.41\cdot 10^{-8}\sqrt{\frac{T}{300}}\exp\left(\frac{22.13\cdot 10^{-3}}{k_B T}\right)$	$2.79\cdot 10^{-8}\sqrt{\frac{T}{300}}\exp\left(-\frac{22.13\cdot 10^{-3}}{k_B T}\right)$
H(195K)	E_T-E_V=0.351eV	$9.85\cdot 10^{-9}\sqrt{\frac{T}{300}}\exp\left(-\frac{85\cdot 10^{-3}}{k_B T}\right)$	$4.3\cdot 10^{-9}\sqrt{\frac{T}{300}}$

Table 2: Recombination center properties

an appropriate simulation of such devices [3,14].

For all simulations, the 2D device simulator TeSCA has been used [2]. This simulation system solves the three fundamental semiconductor equations (the Poisson equation as well as the electron and hole current continuity equation). For the consideration of deep traps, additional terms are necessary. In the Poisson equation (1), the charged recombination centers are considered. In the continuity equations, the thermal capture and emission processes of carriers via the deep levels within the band gap lead to additional recombination terms in the equations (2) and (3). The occupancies of the acceptor or donor traps are evaluated from the balance equations (4) and (5).

$$-\mathrm{div}(\varepsilon\cdot \mathrm{grad}\varphi) = q\left[p - n - N_A^- + N_D^+ + \Sigma\left(N_{TD}^+ - N_{TA}^-\right)\right] \quad (1)$$

$$\frac{\partial n}{\partial t} - \mathrm{div}\, J_n = G - R + \Sigma\left[e_{nA}N_{TA}^- - c_{nA}\, n\left(N_{TA} - N_{TA}^-\right)\right] + \Sigma\left[e_{nD}\left(N_{TD} - N_{TD}^+\right) - c_{nD} n N_{TD}^+\right] \quad (2)$$

$$\frac{\partial p}{\partial t} + \mathrm{div}\, J_p = G - R + \Sigma\left[e_{pA}\left(N_{TA} - N_{TA}^-\right) - c_{pA} p N_{TA}^-\right] + \Sigma\left[e_{pD}N_{TD}^+ - c_{pD}\, p\left(N_{TD} - N_{TD}^+\right)\right] \quad (3)$$

$$\frac{df_A}{dt} = \left(c_{nA}\, n + e_{pA}\right)\left(1 - f_A\right) - \left(c_{pA}\, p + e_{nA}\right)f_A \quad (4)$$

$$\frac{df_D}{dt} = \left(c_{pD} p + e_{nD}\right)\left(1 - f_D\right) - \left(c_{nD} n + e_{pD}\right)f_D \quad (5)$$

Based on this extended recombination model, the behavior of radiated devices is predicted with qualitatively and quantitatively good results [10,11,12].

RECOMBINATION CENTER DATA

For simulation purposes it is necessary not only to implement an appropriate recombination model but also to know the parameters of the radiation-induced centers as well as their temperature dependencies. Even though a lot of publications deal with recombination center parameter determination [1,4-6,13,15], reliable data were not available until recently due to the sophisticated and therefore fault sensitive character of the necessary measurements.

Table 2 shows the center properties as used in the simulations according to previous work [11,12]. There, the fundamental properties of the radiation-induced centers are determined by DLTS measurements [7]. Due to the applied annealing step, the center E(90K) controls the high-level lifetime.

Power devices are usually operated at high injection levels in on-state and turn-on/turn-off. Therefore, it is necessary to know the parameters of E(90K) exactly to allow correct simulations. Since the electron capture rate is small compared to the hole capture rate of E(90K), it is possible to use measurements of the high-level lifetime for an estimation of the temperature-dependent electron capture rate.

These measurements are based on the well-known OCVD (Open Circuit Voltage Decay) technique [8]. Due to the comparatively shallow energetic position of E(90K) within the bandgap of silicon, optical excitation of carriers by means of laser light pulses was used to generate a large density of excess carriers to fulfill the high-injection condition [12].

The composition of the recombination centers detected in electron-radiated silicon depends on the irradiation

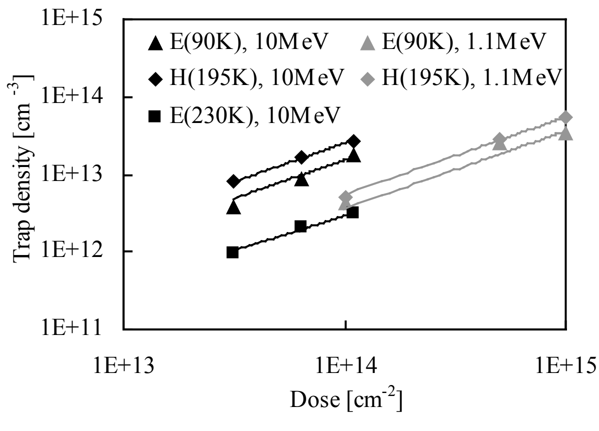

Figure 2: Trap density vs. parameters of electron irradiation

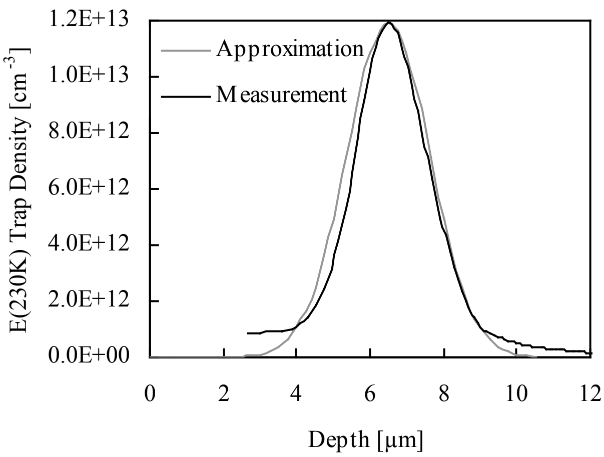

Figure 3: Recombination center profile of E(230K) after additional annealing of type H

parameters. Figure 2 shows the dependence of the trap density on electron energy and dose. In case of low irradiation energy, E(230K) is not detectable. This recombination center already vanished due to the annealing process. Under the applied conditions, the dependence of the generated centers is approximately linear to the irradiation dose.

DLTS measurements were also used for the determination of the concentration profiles in the helium radiated samples. Due to the high concentrations, an additional second annealing step was necessary to allow the profile measurement of E(230K) to be performed.

Figure 3 shows the determined center distribution and the approximation based on a simple gaussian profile as used in the device simulations. For the traps H(195K) and E(90K), the same profile is assumed. The peak concentrations of these traps are approximated from the comparison of the results of lifetime measurements and measurements of the DLTS- and junction capacitance at the helium radiated sample with and without an additional annealing step.

THE INFLUENCE OF LIFETIME CONTROL ON DEVICE PROPERTIES

Forward Characteristics

Figure 4 shows the forward characteristics of the different types E (electron irradiation), H (helium irradiation) and EH (combination of the electron irradiation of type E and the helium irradiation of type H) as a result of simulation and measurement. Beside a satisfying agreement between measurement and simulation results, figure 4 clearly indicates the influence of the different lifetime profiles on the forward voltage characteristics.

Figure 5 shows the impact of the temperature on the forward voltage at nominal current. This temperature dependence is strongly influenced by the properties of the recombination centers, due to the temperature dependent capture rates of the dominant recombination center E(90K). The comparison of the measured and simulated characteristics of type E shows a good accordance. The deviations in case of the types H and EH are most probably caused by the uncertainties of the recombination center profile measurements. Due to the higher forward voltage drop in type EH, other effects, like self-heating caused by recombination heat, may cause an additional error.

Apart from this, figure 5 shows the change in the temperature coefficient due to the different irradiation types. Therefore, lifetime control offers a possibility to tune the temperature coefficient. This is important since a positive temperature coefficient simplifies the paralleling of power devices.

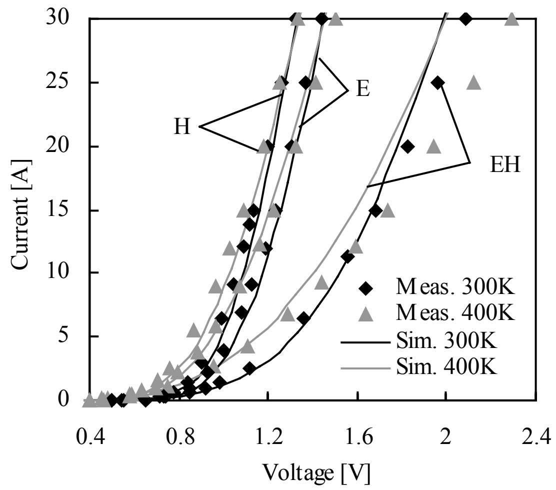

Figure 4: Forward characteristics of types H, E and EH

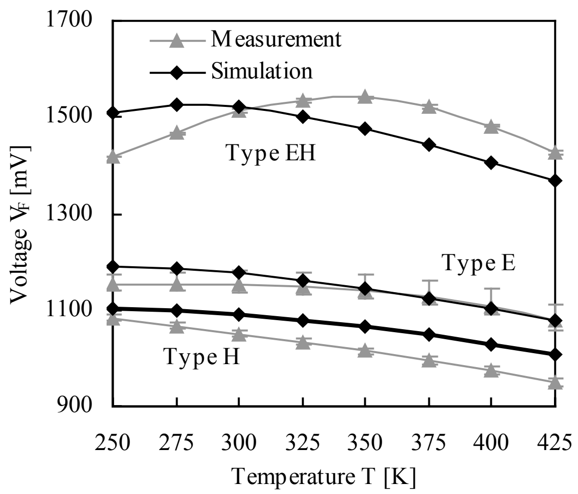

Figure 5: Forward voltage dependence on temperature (I_F=10A)

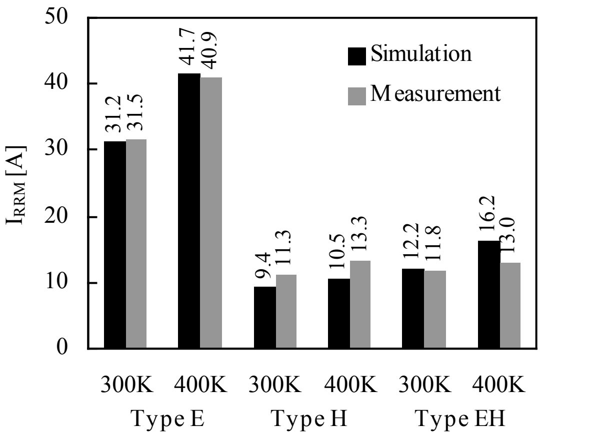

Figure 6: I_{RRM} comparison (V_R=250V, I_F=10A, di/dt=500A/µs)

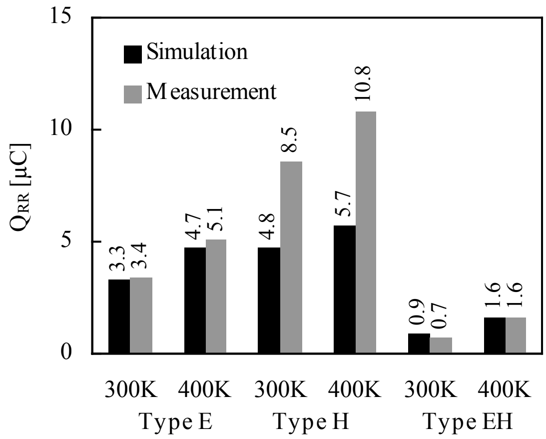

Figure 7: Q_{RR} comparison (V_R=250V, I_F=10A, di/dt=500A/µs)

Turn-Off Characteristics

Figure 6 gives a comparison of the reverse recovery current peak I_{RRM} for the different types E, H and EH. Figure 7 shows the comparison of the stored charge Q_{RR}. As in case of the forward voltage dependencies, the figures give clear evidence to the effects of the different irradiation processes. Obviously, type EH offers the best properties with respect to a low reverse recovery current peak I_{RRM} and the lowest stored charge Q_{RR}.
Under common operating conditions, a sinusoidal current lower than nominal current is often switched in usual topologies. Due to the reduced number of stored carriers in the low-doped region of the freewheeling diode, this is a critical condition for the device. As on example of type E, shown in figure 8, low current may cause a snap-off in the reverse current. This leads to overvoltages and/or oscillations due to parasitic inductances. The use of device simulation offers a opportunity to avoid such a device behavior.

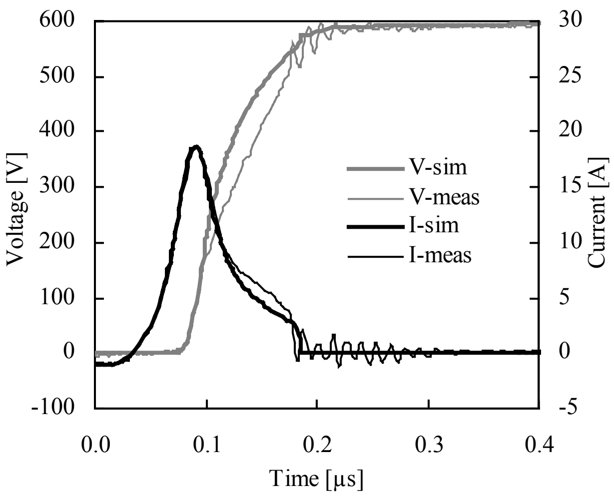

Figure 8: Snap-Off in reverse recovery of type E at low current (V_R=600V, I_F=1A, di/dt=500A/µs)

The Influence of Recombination Center Peak Position

If local lifetime adjustment is applied, the peak position x_p-x_j of the recombination center profile, as illustrated in figure 9, controls the trade-off between forward losses and the stored charge as well as the trade-off between forward losses and reverse recovery current maximum. Figure 10 shows the trade-off between forward voltage drop and the reverse recovery current maximum in dependence of the peak position. Figure 11 shows the trade-off between forward losses and stored charge in dependence of the recombination center peak position as a result of device simulation. Both dependencies have a minimum at a recombination center peak position close to the pn-junction.

Dynamical Effects

Furthermore, device simulation holds potential to avoid disturbing dynamical effects. As an example, figure 12

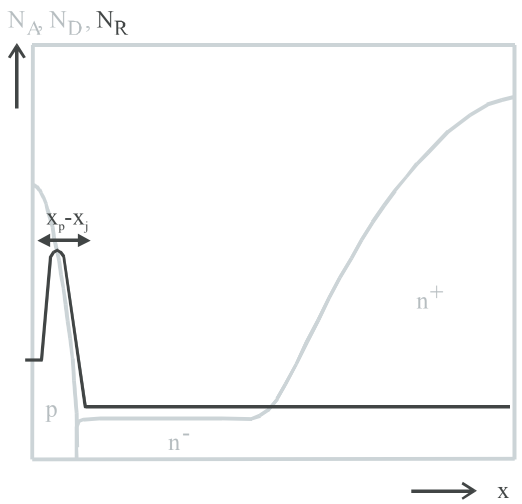

Figure 9: Doping and schematical recombination center profile

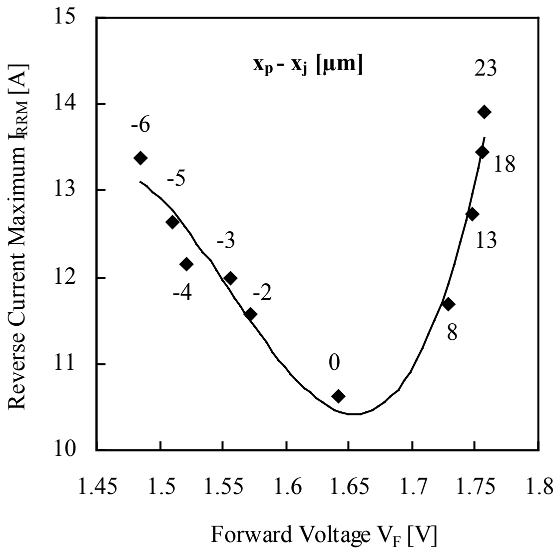

Figure 10: Trade-off between the forward voltage drop and reverse recovery current maximum in dependence of the recombination center peak position

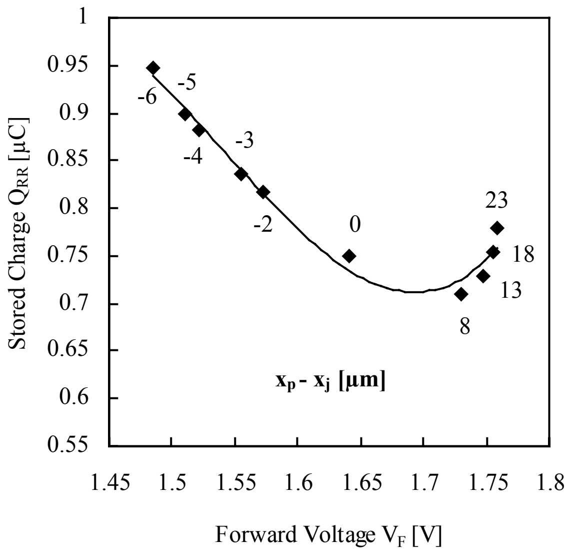

Figure 11: Trade-off between the forward voltage drop and stored charge in dependence of the recombination center peak position

shows the reverse recovery measurement of type E45, where Impatt oscillations appear. The measurement was done using a conventional double-pulse method.

The oscillations are caused by the temporarily positively charged donors H(195K) which reduce the reverse blocking capability. Therefore, avalanche breakdown occurs at the pn-junction region and generates electrons. These electrons counterbalance the positive donors and hence stop the avalanche generation of carriers. Due to the electric field, the electrons are transported to the nn^+-junction and again, avalanche generation starts at the pn-junction. The impatt oscillations stop as soon as the positive donors are discharged and the device is again able to withstand the reverse voltage [9].

For simulation purposes, we used an emulation of the measurement setup. The simulation circuit consisted of the discrete freewheeling diode, a timevariable serial resistance instead of the IGBT and a small inductance.

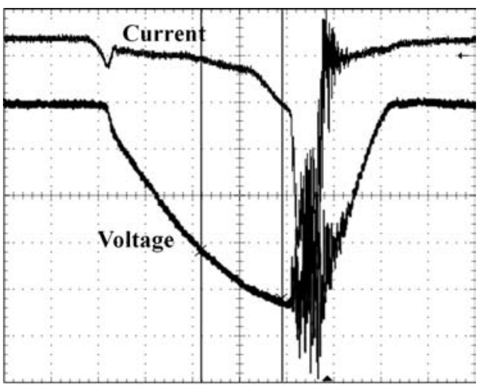

Figure 12: Oscillogramm of temporary impatt oscillation Type E45, $d=1E15cm^{-2}$, T=280K, V_R=910V, I_F=5A (20A/div, 200V/div, 200ns)

This emulation was used to decrease the necessary computing time since only the diode has to be considered. Figure 13 shows a simulation of type E45 (electron dose $d=1E15cm^{-2}$) where impatt oscillations are observed. Figure 14 shows the electron carrier distribution at different times as a result of device simulation to exemplify the physical processes in the device.

The avoidance of these high-frequency oscillations is necessary because of their adverse influence on the drive control units and because of EMC (electromagnetic compability) issues. Furthermore, in some cases the devices were destroyed due to impatt oscillations.

According to previous work [9], the threshold voltage of the impatt oscillation mainly depends on the concentration of the donor-state H(195K), the reverse voltage and the

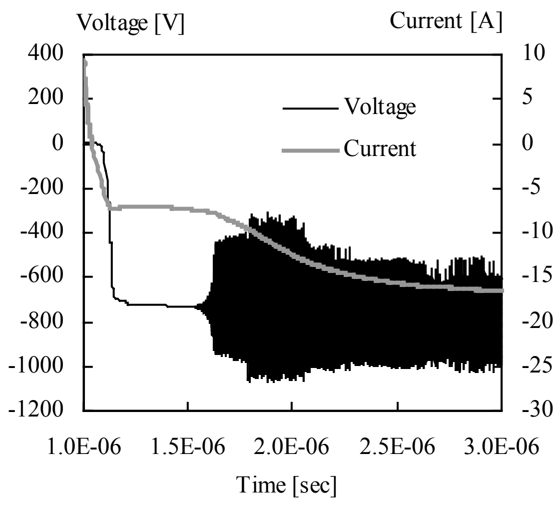

Figure 13: Simulation of temporary impatt oscillation Type E45, $d=1E15cm^{-2}$ (T=270K, V_R=800V, I_F=10A)

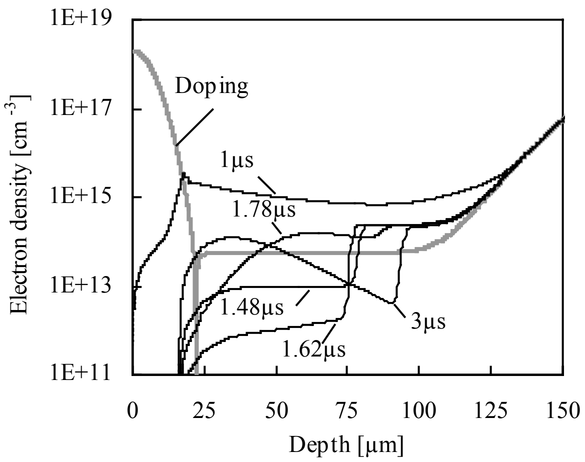

Figure 14: Electron distribution for different points in time during impatt oscillation
Type E45, d=1E15cm^{-2} (T=270K, V_R=800V, I_F=10A)

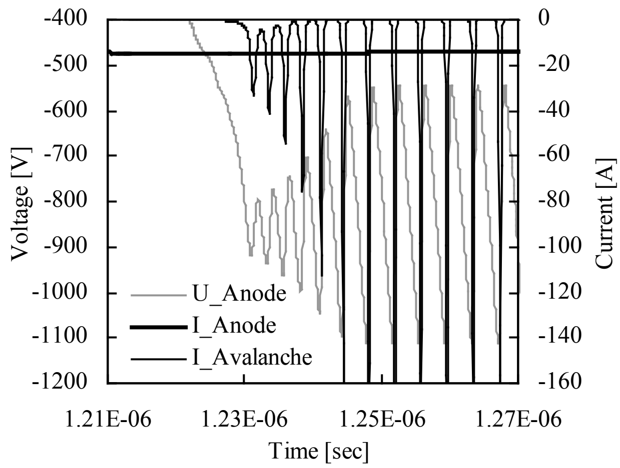

Figure 15: Current and voltage at beginning of impatt oscillation
Type E45, d=5.4E14cm^{-2} (T=250K, V_R=800V, I_F=10A)

temperature.
Figure 16 shows the threshold voltage V_{DI} of type E45 in dependence of temperature for two different irradiation doses. The measured values from [9] are compared with simulation results. For the first time, the temperature dependency of the impatt oscillation can be simulated. Thus, Figure 16 indicates the potential of the device simulation if deep centers are considered.

CONCLUSION

To consider lifetime killing effects in device simulation, the use of an extended recombination model including full trap dynamics is necessary. The introduction of several recombination centers with different properties into simulation allows the correct description of recombination processes under different conditions.
The previously determined center parameters, which were used for simulations, explain the temperature dependencies of stationary and dynamical characteristics.
Based on these results, device simulation is used as a tool for device design. The influence of different recombination center profiles on the stationary and dynamical properties of freewheeling diodes is studied.
It is shown that the optimal position of the recombination center peak is located close to the pn-junction.
Furthermore, the physically correct description of the trap dynamics allows an appropriate simulation of dynamical impatt oscillations for the first time. This effect is caused by temporarily positively charged donor-states which reduce the blocking capability of the device. The consideration of the donor-states is necessary in case of high-dose electron, proton or helium ion irradiation to prevent high-frequency oscillations.
Therefore, device simulation may be used as a powerful tool in the development and optimization of power devices as well as in the explanation of their behavior.

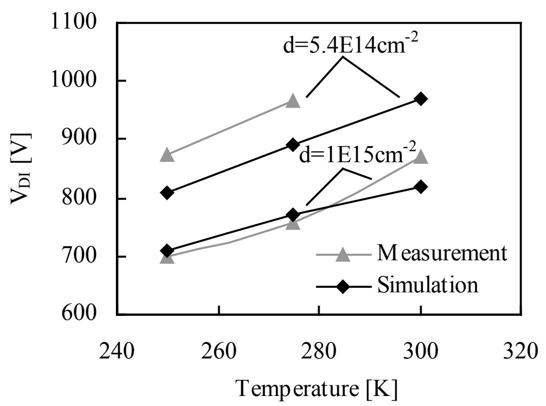

Figure 16: Threshold voltage of impatt oscillation for 4.5MeV electron radiated devices. Measured values from [9]

ACKNOWLEDGEMENTS

The authors wish to thank the scientists, especially Dr. Nürnberg and Prof. Gajewski, from the Weierstrass Institute for Applied Analysis and Stochastics in Berlin, who developed the device simulator TeSCA. Moreover, the authors are grateful for their support and the addition of new features and algorithms into the simulation system.
The Authors would like to thank also Ms. Pellkofer and Mr. Umland for their support in sample preparation and measurement assistance.
We also wish to thank Prof. Wagemann from the Technical University of Berlin for the opportunity to perform DLTS measurements.
This work has been supported by grants of the Deutsche Forschungsgemeinschaft.

REFERENCES

[1] Bleichner, H., Jonsson, P. and Keskitalo, N.: Temperature and injection dependence of the Shockley-Read-Hall-lifetime in electron irradiated n-type silicon, Journal of Applied Physics, 79(12), 1996, 9142-9148

[2] Gajewski, H., Heinemann, B. and Langmach, H.: *TeSCA-Handbuch*, Weierstrass-Institute for Applied Analysis and Stochastics Berlin, 1991

[3] Hazdra, P. and Vobecký, J.: Accurate Simulation of Fast Ion Irradiated Power Devices, Solid-State Electronics, 37(1), 1994, 127-134

[4] Hüppi, M. W.: *Protonenbestrahlung von Silizium: Vollständige elektrische Charakterisierung der erzeugten Rekombinationszentren*, Dissertation ETH Zürich, 1989

[5] Irmscher, K.: *Kapazitätsspektroskopische Analyse tiefer Störstellen in ionenimplantiertem Silizium*, Dissertation Humboldt-University of Berlin, 1985

[6] Keskitalo, N.: *Irradiation Induced Defects for Lifetime Control in Silicon*, Dissertation Uppsala University, 1997

[7] Lang, D.V.: Deep-Level Transient Spectroscopy: A New Method to Characterize Traps in Semiconductors, Journal of Applied Physics, 45(7), 1974, 3023-3032

[8] Lederhandler, S.R. and Giacoletto, L.J.: Measurement of Minority Carrier Lifetime and Surface Effects in Junction Devices, Proc. IRE (1955), 477-483

[9] Lutz, J., Südkamp, W. and Gerlach, W.: Impatt Oscillations in Fast Recovery Diodes due to Temporarily Charged Radiation-Induced Deep Levels, Solid-State Electronics, 42(6), 1998, 931-938

[10] Siemieniec, R., Südkamp, W. and Lutz, J.: Simulation and Experimental Results of Radiation Induced Traps in Silicon, Proc. EPE'99 (Lausanne 1999)

[11] Siemieniec, R., Südkamp, W. and Lutz, J.: Applying Device Simulation for Lifetime-Controlled Devices", Proc. ICCDCS 2002 (Aruba 2002)

[12] Siemieniec, R., Südkamp, W. and Lutz, J.: Determination of Parameters of Radiation Induced Traps in Silicon, Solid-State Electronics, 46(6), 2002, 891-901

[13] Südkamp, W.: *DLTS-Untersuchung an tiefen Störstellen zur Einstellung der Trägerlebensdauer in Si-Leistungsbauelementen*, Dissertation Technical University of Berlin, 1994

[14] Wertheim, G.K.: Transient Recombination of Excess Carriers in Semiconductors, Physical Review, 100(4), 1958, 1086-1091

[15] Wondrak, W.: *Erzeugung von Strahlenschäden in Silizium durch hochenergetische Elektronen und Protonen*, Dissertation University Frankfurt/M., 1985

Addresses of the authors

Ralf Siemieniec, Technical University of Ilmenau, Dept. of Solid-State Electronics, P.O. Box 100565, D-98684 Ilmenau, Germany, e-mail: ralf.siemieniec@tu-ilmenau.de

Josef Lutz, Technical University of Chemnitz, Faculty of Electrical Engineering and Information Technology, D-09107 Chemnitz, Germany, e-mail: josef.lutz@infotech.tu-chemnitz.de